

## **SILICA-BASED PHOTONIC CRYSTAL FIBER FOR SUPERCONTINUUM GENERATION IN THE ANOMALOUS DISPERSION REGION: MEASUREMENT AND SIMULATION**

BIEN CHU VAN<sup>1</sup>, HIEU VAN LE<sup>2,†</sup>, CHIN HOANG VAN<sup>2</sup>, THAO NGUYEN THI<sup>2</sup>, VAN THUY HOANG<sup>3</sup>, QUANG HO DINH<sup>4</sup> AND VAN CAO LONG<sup>5</sup>

<sup>1</sup>*Yersin Da Lat University, 27 Ton That Tung, Ward 8, Da Lat City, Vietnam*

<sup>2</sup>*Faculty of Natural Sciences, Hong Duc University, 565 Quang Trung Street, Thanh Hoa City, Vietnam*

<sup>3</sup>*Department of Physics, Vinh University, 182 Le Duan, Vinh City, Vietnam*

<sup>4</sup>*School of Chemistry, Biology and Environment, Vinh University, 182 Le Duan Street, Vinh City, Vietnam*

<sup>5</sup>*Institute of Physics, University of Zielona Góra, Prof. Szafrana 4a, 65-516 Zielona Góra, Poland*

*E-mail:* <sup>†</sup>[levanhieu@hdu.edu.vn](mailto:levanhieu@hdu.edu.vn)

*Received 26 May 2022; Accepted for publication 25 July 2022; Published 9 August 2022*

**Abstract.** *We report on numerical simulation and experimental study of the supercontinuum (SC) generation in the anomalous dispersion region of photonic crystal fiber (PCF). The results show that a flat and stable spectrum with bandwidth of 130 nm around the central pump wavelength was achieved with an input power of 4.0 W. Although the measured spectrum is slightly different from the numerical ones, a good consistency can be recognized in the major sideband positions and spectral width. In addition, the chromatic dispersion of air silica PCF was measured at visible and near-infrared wavelengths using the Mach-Zehnder interferometer configuration and then verified by comparison with simulated results.*

**Keywords:** nonlinear optics; photonic crystal fiber; anomalous dispersion; supercontinuum generation.

**Classification numbers:** 42.65.Jx; 42.55.Tv; 63.20.D.

### **I. INTRODUCTION**

Supercontinuum (SC) generation in photonic crystal fibers (PCFs) has attracted extensively due to their outstanding applications. They include, for instance, in spectroscopy, frequency metrology, optical coherence tomography, chemical detection, and biomedicine [1–4]. For those

applications, it is important to know optical properties of the generated continuum signals like the spectral width and the coherency. In general, the spectral broadening normally results from the interplay between the dispersion properties and nonlinearity of the waveguide, incorporating with the formation of optical solitons. Meanwhile, the coherence property of SC spectra depends on the parameters of the pump light and spectral broadening mechanism. To obtain coherent SC light sources, PCFs having all normal dispersion (AND) profile are also commonly used as the nonlinear media [5, 6]. In the AND region, self-phase modulation (SPM) and then optical wave breaking (OWB) are responsible for the expansion of the output spectrum, although the expanded bandwidth is often limited [5].

The coherent properties of SC light can also be obtained by controlling the input soliton number using a pumping wavelength which is closed to the zero-dispersion wavelength (ZDW) in the anomalous dispersion (AD) region of PCFs. In this region, the spectral broadening of the output pulse is created mainly due to nonlinear effects associated with soliton fission and dispersive waves [7, 8]. Besides that, the soliton dynamics are sensitive to input pulses [7]. Small changes in the input pulse parameters can lead to a complex temporal profile of output spectra and an increase in noise [8], consequently, limiting practical applications of the generated SC sources [9]. However, overcome that drawback, a broadening and highly coherent of SC spectra produced in AD region with lower peak power brings the great advantage for nonlinear integrated photonic devices. That is why the SC generation in the AD regime has been extensively studied; their performance in terms of spectral flatness, bandwidth and the coherent SC spectrum still needs further optimization.

Recently, there have been a number of experiments and simulations demonstrating SC generation in the AD region of PCFs [10–14]. Li *et al.* reported a study on the coherency of SC spectra of a tapered fluorotellurite micro-structured fiber in wavelength range of 1.4 to 4  $\mu\text{m}$  with pumped wavelength of 1980 nm [10]. Y. Huang *et al.* numerically analyzed SC generation in PCFs both normal and AD regions. Fiber considered there has flat dispersion with three ZDWs. In that work, they used a pump wavelength in the AD region to generate a wide, flat, and coherent SC spectrum with a wavelength range from 1281 nm to 2200 nm [11]. Park *et al.* reported a numerical generation of SC spectra in a rare-earth-doped highly nonlinear PCF with AD regime in the sub-picosecond pulse regime [12]. F.R.A. Sierra *et al.* investigated the dynamics of cascading solitons in fiber amplifiers using the complex Ginzburg-Landau equation [13]. In this case, each input pulse allowed the generations of multiple ultrashort pulses of different wavelengths at the amplifier output. On the other hand, the number of pulses depends on the total gain of the amplifier as well as on the input pulse width. C. Lei *et al.* numerically investigated SC generation in a nonlinear ytterbium-doped fiber amplifier with an AD region [14]. By pumping at the wavelength of 1060 nm and an output power of 300 W, a broad SC spectrum was obtained in the wavelength range from 1000 nm–2000 nm. In the above mentioned studies, the fiber is almost made of non-silica glass and incorporates a used laser source pump at long wavelengths such as 1400 nm, 1660 nm. Meanwhile, silica glass is the most versatile material, as it ensures a wide transmission window with low loss from the near-ultraviolet to infrared (IR) range, and glass purity [15], still has not been considered much in the AD region.

In this paper, we report the experimental and numerical results of the SC generation of the PCF in the AD region. The tested fiber based on silica glass having 7 rings of air holes ordered in regular hexagonal lattice with a solid core. Firstly, the tested-fiber dispersion characteristics

was numerically simulated based on its cross-section of scanning electron microscope (SEM) images and then verified experimentally using the Mach-Zehnder interferometric technique. Next, SC generation was experimentally investigated and compared with the theoretical calculations using the generalized nonlinear Schrödinger equation (GNLSE). The results demonstrate that SC spectrum having a stable and flat were obtained within the wavelength range of 960 nm -1090 nm when the input power 4.0 W is applied.

## II. FIBER LAYOUT DESIGN AND DISPERSION MEASUREMENT

### III. Development of the PCF

In our work, the designed PCF is made of silica glass using the stack and draw technique. The manufacturing process consists of two main stages. First, a sub-preform was stacked from capillary tubes and rods and the initial drawing was made with the low pressure to close the gaps between capillaries and rods. Second, the final PCF structure was drawn from the sub-preform, where a selective choice of pressure and temperature reduced the size of capillaries to the size of the designed PCF structure. The PCF was fabricated at the Institute of Electronics Materials Technology (ITME), Poland. The cross-section of the fiber is shown in Fig.1. The silica fiber has a solid core with the diameter of  $5.024 \mu\text{m}$ . The lattice constant  $\Lambda$  between air holes is  $3.256 \mu\text{m}$ , the filling factor  $d/\Lambda = 0.457$  in the first ring. Meanwhile, the remaining outer rings, the filling factor ranging between 0.37 and 0.52. The refractive index silica glass as a function of wavelength is given by the Sellmeier equation as:

$$n(\lambda) = \sqrt{1 + \frac{B_1\lambda^2}{\lambda^2 - C_1} + \frac{B_2\lambda^2}{\lambda^2 - C_2} + \frac{B_3\lambda^2}{\lambda^2 - C_3}} \quad (1)$$

where  $B_1 = 0.6694226$ ,  $B_2 = 0.4345839$ ,  $B_3 = 0.8716947$ ,  $C_1 = 0.0044801 \mu\text{m}^2$ ,  $C_2 = 0.013285 \mu\text{m}^2$ ,  $C_3 = 95.341482 \mu\text{m}^2$  are Sellmeier coefficients and  $\lambda$  is the wavelength [16].

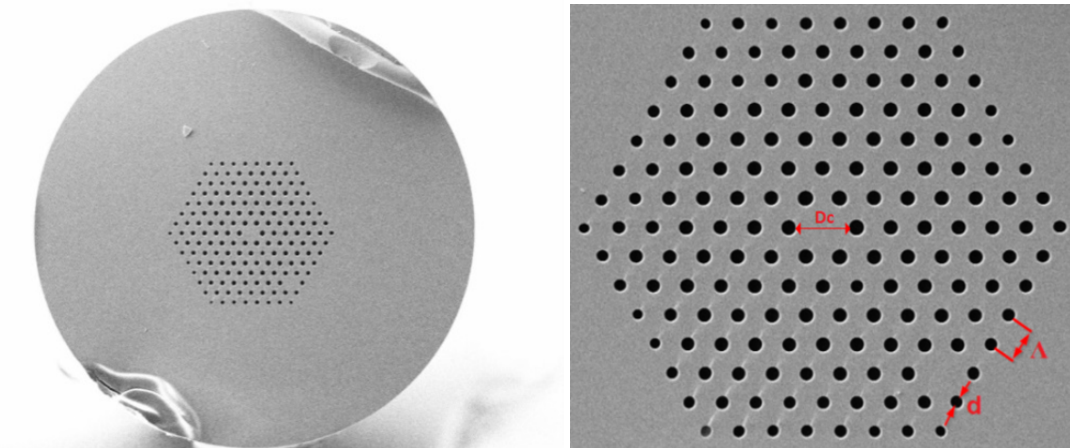


**Fig. 1.** The SEM images of the fabricated PCF.

### III.1. Measurement of the characteristics dispersion

The dispersion property of the fiber consists of the waveguide and the material dispersions, which is expressed by the parameter  $D$  as follows [17]:

$$D(\lambda) = -\frac{\lambda}{c} \frac{d^2 Re(n_{eff})}{d\lambda^2} \quad (2)$$

where  $Re(n_{eff})$  is the real part of refractive index of the propagating mode.

The dispersion characteristics of the test PCF are measured using a Mach-Zehnder interferometer setup [18] as presented in Fig. 2. In this case, we used the laser source (SuperK Compact) emitting the light at a wavelength range of 400-2000 nm. In accordance, the detection was performed by two spectrometers: a Thorlabs Compact Spectrometer CCS175/M operating from 0.4 to 1.1  $\mu\text{m}$  and an Avantes AvaSpec-NIR256-1.7 spectrometer for the wavelength range of 0.9 to 1.7  $\mu\text{m}$ . The length of test silica fiber was used 12.0 cm. In fact, we studied the simulation and experimental method of the zero-dispersion shift in PCFs infiltrated with water-ethanol mixture [19]. However, we used there a PCF with the same structure, for example, background material, number of air hole rings but different in the lattice constant and diameter of air holes in this work.

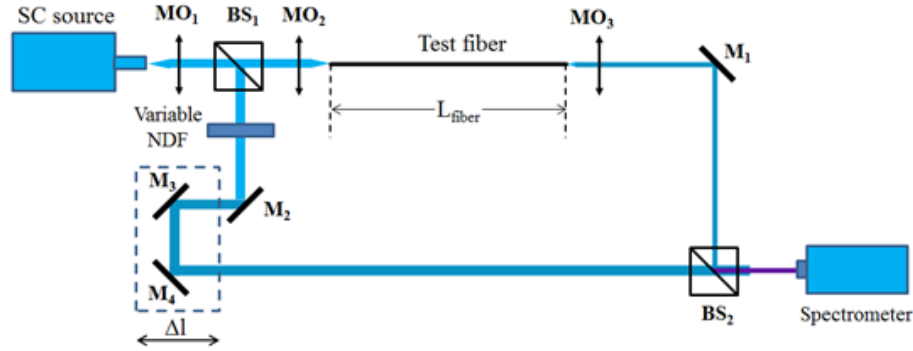
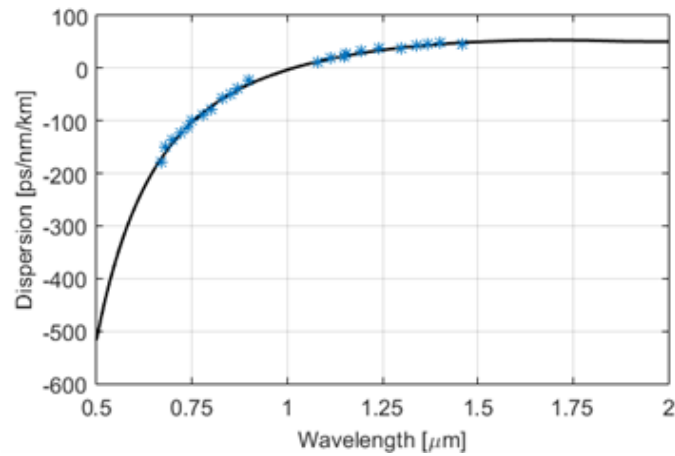


Fig. 2. Mach-Zehnder interferometer setup used to measure dispersion in silica PCFs.

Obtained experimental data along with numerically calculated dispersion profile using real fiber geometric parameters are shown in Fig. 3. The simulation was performed with the helping of the Lumerical Mode Solution software [20] to calculate the dispersion characteristics of the fundamental mode as a function of wavelengths. As results, experimental data and numerical dispersion properties are well matched. Based on this simulation, the ZDW of the PCF is about 1.01  $\mu\text{m}$ , while measured results indicate that ZDW is located at 1.025  $\mu\text{m}$  (with error of 1.5%). Thus, we obtained high correspondence in the location of the ZDW. The slight differences may be due to the inaccuracies of tested-fiber geometrical parameters taken from only a single cross-section image and the approximations in experimental data process.

## IV. SUPERCONTINUUM GENERATION IN THE TEST PCF

In this section, firstly, the SC generation in developed silica PCF was measured using a setup as shown in Fig. 4. In this setup, we used a femtosecond fiber laser emitting 400 fs pulses with the central wavelength of 1.03  $\mu\text{m}$  and 10 MHz repetition rate. The laser pulses from the



**Fig. 3.** Measured and simulation results for chromatic dispersion of the test silica PCF.

SC source are directed into the first lens  $O_1$  by the system of mirrors  $M_1$ . As a result, the laser pulses were coupled into the fiber core and then propagate through the fiber and are collected by the lens  $O_2$  behind the fiber output. Next, the light pulses were reflected by the mirror  $M_2$  and directed to the camera  $C$  to check the coupling quality. After achieving the maximum coupling efficiency, the light was directed into the multimode fiber  $M$  to the spectrometer. In this setup, we used two spectrometers: Thorlabs Compact Spectrometer CCS175/M (ranges 0.4 - 1.1  $\mu\text{m}$ ) and Avantes AvaSpec-NIR256-1.7 (range 0.9 - 1.7  $\mu\text{m}$ ) to record the spectral output of SC generation. Note that the fiber length used in this experiment was 12.0 cm.

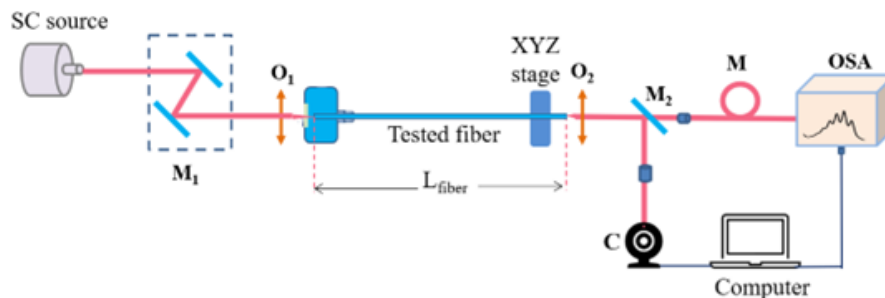


**Fig. 4.** Schematic of the measurement for SC generation in the tested silica PCF.

The experimental results of the SC spectra in the test silica fiber for various input powers are presented in Fig. 5. The broadening of the SC spectrum occurs symmetrically around the central wavelength of 1030 nm. Besides that increasing the input laser power causes SC spectral broadening. For example, for the case of input laser power is 3.0 W, broad SC spectrum is spanned in the wavelength range of 970 nm - 1080 nm. Meanwhile, the input laser power is increased to about 4.0 W, the SC spectrum is extended to a wider range spanning in the wavelength range

of 960 nm -1090 nm. Because of the limited measuring range of the spectrometer we used, the measured SC spectrum is shown only up to 1100 nm. Due to the pump wavelength (1030 nm) is in the AD region, SPM, soliton fission and then FWM effect dominated during the process of SC generation. Although the spectral bandwidth is not very wide, the stable and high-flatness SC spectra were achieved.

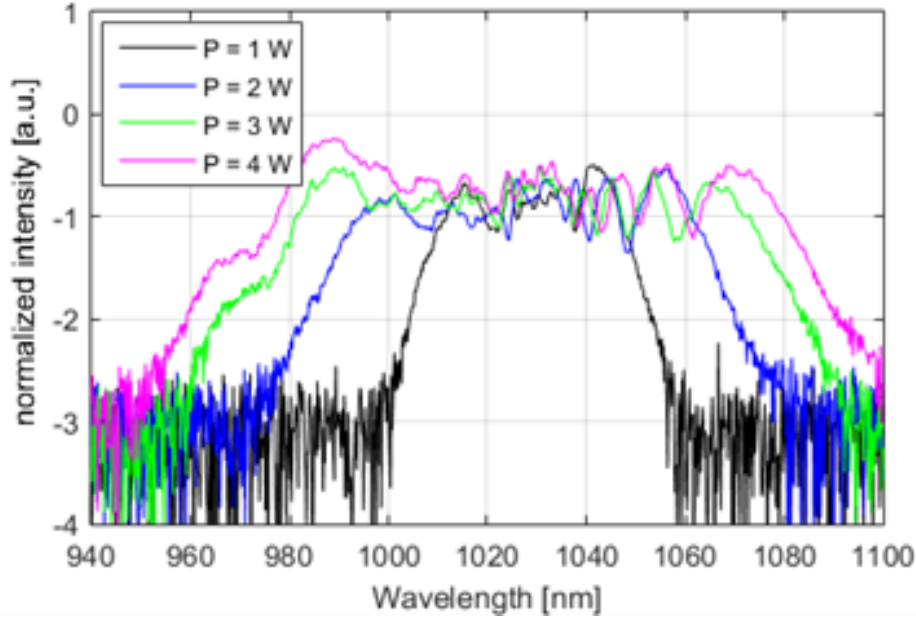


**Fig. 5.** Measurement of output spectra in the tested silica PCF with different power of the laser source.

Next, we numerically modeled SC generation in the tested silica PCF to verify the experimental data. In order to achieve these goals, we solved the GNLSE using the Split-Step Fourier method [17]. This equation has the following form:

$$\begin{aligned} \frac{\partial A}{\partial z} = & -\frac{\alpha}{2}A + \sum_{n \geq 2} \beta_n \frac{i^{n+1}}{n!} \frac{\partial^n}{\partial T^n} A \\ & + i\gamma \frac{1}{\omega_0} \left(1 + \frac{\partial}{\partial T}\right) \left[ (1 - f_R)|A|^2 A + f_R A \int_0^\infty h_R(t) |A(z, T-t)|^2 dt \right] \end{aligned} \quad (3)$$

where  $A = A(z, t)$  presents the complex amplitude of the optical field.  $\alpha$  is the fiber loss. The nonlinear coefficient is  $\gamma = n_2 \omega_0 / c A_{\text{eff}}$ , where  $n_2 = 2.74 \times 10^{-20} \text{ m}^2 \text{ W}^{-1}$  is the nonlinear refractive index of silica glass [17] and  $A_{\text{eff}}$  is the effective modal area of the fiber.  $\lambda_c$  denote the center wavelength.  $\beta_n$  are coefficients of the Taylor series expansion of the propagation constant around the carrier frequency,  $f_R$  is the fractional contribution of the Raman response to the nonlinear polarization, while,  $h_R(t)$  represents the Raman response function, and was approximated with a standard damped oscillator model,  $h_R(t) = (\tau_1^2 + \tau_2^2) \tau_1^{-1} \tau_2^{-2} \exp(-t/\tau_2) \sin(t/\tau_1)$ .

In the simulation, we assumed that a commercially available fiber based femtosecond laser emitting with pump wavelength of  $1.03 \mu\text{m}$ , the pulse duration of 400 fs and 12.0 cm fiber length. The Gaussian pulse is considered as an input pulse. The Raman fraction  $f_R$  of silica fiber is equal to 0.18,  $\tau_1 = 12.2 \text{ fs}$ ,  $\tau_2 = 32 \text{ fs}$  [17]. In this case, at the pump wavelength of 1030 nm, the effective modal area is  $12.74 \mu\text{m}^2$ , the nonlinear coefficient is  $\gamma = 13.12 \text{ W}^{-1}\text{km}^{-1}$ . Since length of test fiber is short to consider in the simulations, the fiber loss is neglected.

Figure 6 shows the comparison between numerical simulations (blue curve) and experimental data (black curve) for the SC generation of silica PCF. As results, although the experimental spectrum is slightly different from the numerical ones, a good consistency can be recognized in the spectral width and major sideband positions.

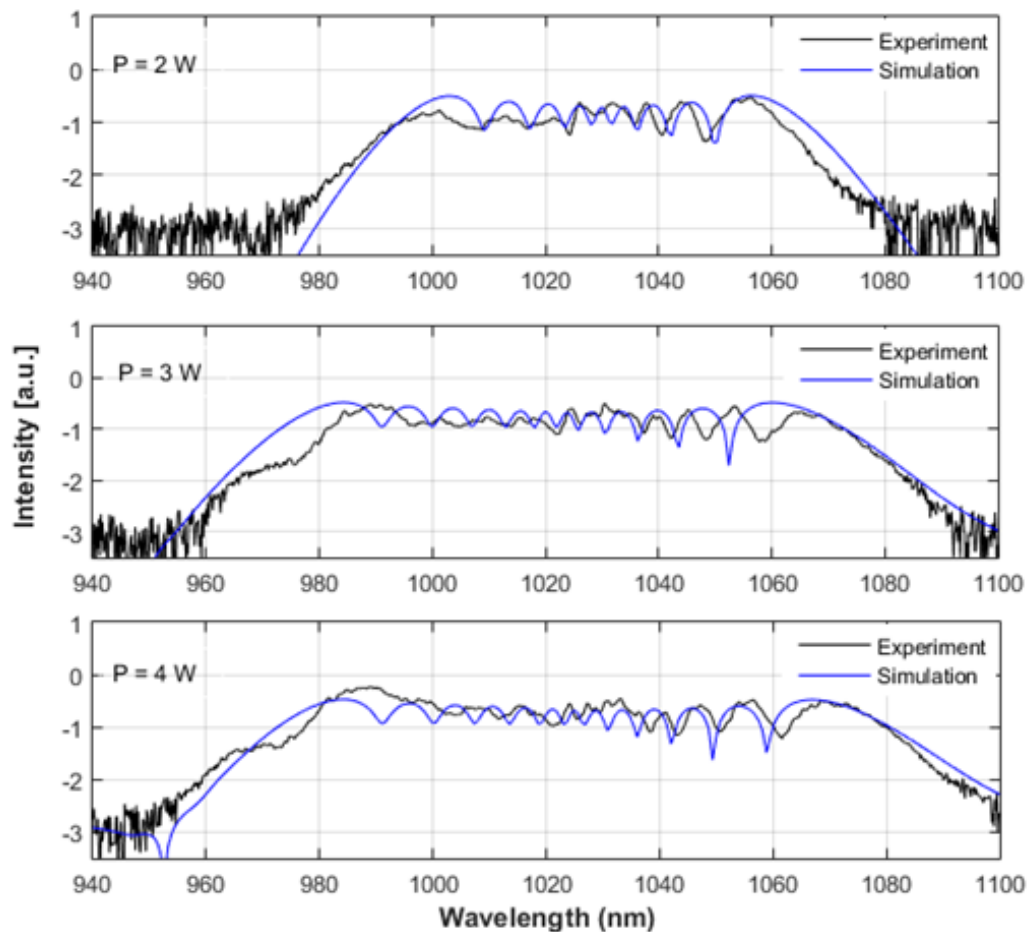


**Fig. 6.** Comparison of experimental and numerical results for the SC generation in the silica-PCF.

**Table 1.** Over-review of experimental results for output spectral width in AD region of PCFs around a central pumping wavelength of 1.03  $\mu\text{m}$ .

Type of fibers	Pump wavelength	Regime	Pulse length	Pulse energy/peak power	Spectral bandwidth (nm)	Refs.
Silica-PCF	1.03 $\mu\text{m}$	AD	400 fs	4.0 W	130	This work
Ytterbium-PCF	1.06 $\mu\text{m}$	AD	9 ps	6.54 W	100	[14]
Silica-fiber	1.08 $\mu\text{m}$	AD	300 fs	0.3 W	51	[21]
Yb-fiber	1.03 $\mu\text{m}$	AD	50 fs	5.0 nJ	70	[22]

## V. CONCLUSIONS

We presented experimental and numerical results of the SC generation in the AD region of silica PCF. The flat and stable spectrum with bandwidths of 130 nm around the central pumping wavelength was achieved with input power of 4.0 W. Because the pump wavelength is close to the AD region, SPM, Raman scattering and FWM effect dominated during the process of SC generation. In addition, increasing the input power causes pulse spectral broadening. Although, the experimental spectrum is slightly different from the numerical ones, a good consistency can be recognized in the spectral width and major sideband positions. The chromatic dispersion measurements of the silica PCF were made based on the Mach-Zehnder interferometer. Our simulations were conducted with input parameters taken from SEM image of the real fabricated fiber structure and showed good agreement with the experimental results. The slight differences may be due to the inaccuracies of tested fiber geometrical parameters taken from a single cross-section image for calculations and the approximations of experimental data processes. We strongly believe that this study of SC generation of a PCF in the AD region will pave the way to advances in the SC generation technology.

## ACKNOWLEDGEMENT

This research is funded by Vietnam National Foundation for Science and Technology Development (NAFOSTED) under grant number 103.03-2020.19.

## REFERENCES

- [1] T. Stiehm, R. Schneider, J. Kern, I. Niehues, S. Michaelis de Vasconcellos and R. Bratschitsch, *Supercontinuum second harmonic generation spectroscopy of atomically thin semiconductors*, *Rev. Sci. Instrum.* **90** (2019) 083102.
- [2] H. Wang, C. P. Fleming and A. M. Rollins, *Ultra-high-resolution optical coherence tomography at 1.15  $\mu\text{m}$  using photonic crystal fiber with no zero-dispersion wavelengths*, *Opt. Express.* **15** (2007) 3085.
- [3] C. Poudel and C. F. Kaminski, *Supercontinuum radiation in fluorescence microscopy and biomedical imaging applications*, *J. Opt. Soc. Am. B* **36** (2019) A139.
- [4] J. Villatoro, M. P. Kreuzer, R. Jha, V. P. Minkovich, V. Finazzi, G. Badenes *et al.*, *Photonic crystal fiber interferometer for chemical vapor detection with high sensitivity*, *Opt. Express.* **17** (2009) 1447.
- [5] A. M. Heidt, A. Hartung, G. W. Bosman, P. Krok, E. G. Rohwer, H. Schwoerer and H. Bartelt, *Coherent octave spanning near-infrared and visible supercontinuum generation in all-normal dispersion photonic crystal fibers*, *Opt. Express.* **19** (2011) 3775.

- [6] L. E. Hooper, P. J. Mosley, A. C. Muir, W. J. Wadsworth and J. C. Knight, *Coherent supercontinuum generation in photonic crystal fiber with all-normal group velocity dispersion*, *Opt. Express*. **19** (2011) 4902.
- [7] G. Qin, X. Yan, C. Kito, M. Liao, C. Chaudhari, T. Suzuki *et al.*, *Supercontinuum generation spanning over three octaves from UV to 3.85  $\mu\text{m}$  in a fluoride fiber*, *Opt. Lett.* **34** (2009) 2015.
- [8] J. C. Hernandez-Garcia, J. M. Estudillo-Ayala, R. I. Mata-Chavez, O. Pottiez, R. Rojas-Laguna and E. Alvarado-Mendez, *Experimental study on a broad and flat supercontinuum spectrum generated through a system of two PCFs*, *Laser Phys. Lett.* **10** (2013) 075101.
- [9] J. M. Dudley and S. Coen, *Coherence properties of supercontinuum spectra generated in photonic crystal and tapered optical fibers*, *Opt. Lett.* **27** (2002) 1180.
- [10] N. Li, F. Wang, C. Yao, Z. Jia, L. Zhang, Y. Feng *et al.*, *Coherent supercontinuum generation from 1.4 to 4  $\mu\text{m}$  in a tapered fluorotellurite microstructured fiber pumped by a 1980 nm femtosecond fiber laser*, *Appl. Phys. Lett.* **110** (2017) 061102.
- [11] Y. Huang, H. Yang, S. Zhao, Y. Mao and S. Chen, *Design of photonic crystal fibers with flat dispersion and three zero dispersion wavelenghts for coherent supercontinuum generation in both normal and anomalous regions*, *Results in Phys.* **23** (2021) 104033.
- [12] K. Park, J. Na, J. Kim and Y. Jeong, *Numerical study on supercontinuum generation in an active highly nonlinear photonic crystal fiber with anomalous dispersion*, *IEEE J. Quantum Electron.* **56** (2020) 6800109.
- [13] F. R. Arteaga-Sierra, A. Antikainen and G. P. Agrawal, *Dynamics of soliton cascades in fiber amplifiers*, *Opt. Lett.* **41** (2016) 5198.
- [14] C. Lei, A. Jin, R. Song, Z. Chen and J. Hou, *Theoretical and experimental research of supercontinuum generation in an ytterbium-doped fiber amplifier*, *Opt. Express*. **24** (2016) 9237.
- [15] T. Li, *Optical Fiber Communications: Fiber Fabrication*, Academic Press (San Diego), 1985.
- [16] V. C. Lanh, A. Anuskiewicz, A. Ramaniuk, R. Kasztelanic, K. D. Xuan, V. C. Long *et al.*, *Supercontinuum generation in photonic crystal fibres with core filled with toluene*, *J. Opt.* **19** (2017) 125604.
- [17] G. P. Agrawal, *Nonlinear Fiber Optics 5th edition*, Academic Press (Oxford), 2013.
- [18] H. Saghaei, P. Elyasi and R. Karimzadeh, *Design, fabrication, and characterization of Mach-Zehnder interferometers*, *Photonics Nanostructures - Fundam. Appl.* **37** (2019) 100733.
- [19] H. L. Van, R. Buczynski, V. C. Long, M. Trippenbach, K. Borzycki, A. N. Manh *et al.*, *Measurement of temperature and concentration influence on the dispersion of fused silica glass photonic crystal fiber infiltrated with water-ethanol mixture*, *Opt. Commun.* **407** (2018) 417.
- [20] Mode Solution, Lumerical Solutions, <https://www.lumerical.com/tcad-products/mode/>
- [21] S. Ramachandran, S. Ghalmi, J. W. Nicholson, M. F. Yan, P. Wisk, E. Monberg *et al.*, *Anomalous dispersion in a solid, silica-based fiber*, *Opt. Lett.* **31** (2006) 2532.
- [22] F. Ö. Ilday, J. R. Buckley, H. Lim, F. W. Wise and W. G. Clark, *Generation of 50-fs, 5-nJ pulses at 1.03  $\mu\text{m}$  from a wave-breaking-free fiber laser*, *Opt. Lett.* **28** (2003) 0146.